Carbohydrate Research, 214 (1991) 55–69
Elsevier Science Publishers B.V., Amsterdam

Hydrolysis of xanthan in dilute acid: Effects on chemical composition, conformation, and intrinsic viscosity*

Bjørn E. Christensen† and Olav Smidsrød
Norwegian Biopolymer Laboratory (NOBIPOL), Division of Biotechnology, University of Trondheim, NTH, N-7034 Trondheim (Norway)

ABSTRACT

The polysaccharide xanthan has been depolymerized by mild acid hydrolysis (pH 1–4) at 80°. The conformational state was varied from fully ordered to partially disordered by varying the ionic strength and pH. Hydrolysis occurred mainly in the side chains, with the terminal β-mannose as the most susceptible unit, yielding a continuous series of modified xanthans from the intact "polypentamer" to the "polytetramer", while retaining a high molecular weight. Depolymerization of the glucan backbone was analysed by monitoring the intrinsic viscosity ([η]). For ordered xanthan the calculated changes in the degree of polymerization (x_w) as a function of time deviate strongly from that expected for random depolymerization of a single-stranded, linear polymer, but the data are in qualitative agreement with the behaviour of such double-stranded polymers as DNA. The conformational properties of partly hydrolysed xanthan were investigated by optical rotation. For the series degraded at pH 2, the midpoint of the temperature-driven transition (T_m) was > 95° in all cases, but the absolute value of the specific optical rotation ([α]) increased by increasing hydrolysis time, a change partly ascribed to an increase in the fraction of disordered chains, but also to the loss of β-mannose. This loss itself did not appear to influence the conformational state or the depolymerization rates of the xanthan backbone.

INTRODUCTION

Xanthan, the extracellular polysaccharide produced by the bacterium *Xanthomonas campestris*, is used commercially as viscosifier in a wide variety of applications. In particular, xanthan seems to fulfil the requirements for use in drilling muds and in enchanced oil-recovery processes. Its structure is well known[1]; it consists essentially of a (1→4)-linked β-D-glucan (cellulose) backbone substituted at O-3 of every second glucose residue by the trisaccharide: β-D-Man*p*-(1→4)-β-D-Glc*p*A-(1→2)-α-D-Man*p*-(1→. In addition the side chains may contain varying amounts of *O*-acetyl and pyruvic acetal groups, giving rise to structural heterogeneity. The possibility of unsubstituted regions in the backbone has also been discussed[2].

Xanthan may undergo a temperature-driven order–disorder transition in aqueous solutions. The transition depends on temperature[3–5], ionic strength[6,7], salt type[4,8], and molecular weight[5,9], in addition to the pyruvate and acetate content[10]. The determination of T_m, that is, the mid-point of the transition, also depends upon the method used[11]. Various molecular models have been used in order to describe the different

* Presented at the 15th International Carbohydrate Symposium, Yokohama, Japan, August 12–17, 1990.
† Corresponding author.

0008-6215/91/$ 03.50

conformational states. The stiff, extended form (persistence length 120–150 nm) which is normally observed, is shown to exist in a double-stranded conformation[12,13] whereas the denatured or disordered form observed at low ionic strengths and/or elevated temperatures seems to be[13,14] at least partly single-stranded, with a persistence length of ~60 nm. A star-shaped, dimeric model for partially dissociated xanthan at 80° in 10mM NaCl has also been proposed[7], whereas some groups have concluded that xanthan is single-stranded in all cases[6,15,16]. Recently, kinetic data on the salt-induced ordering of xanthan originally interpreted in terms of a single-stranded structure[9] have been reinterpreted in favour of a partly double-stranded structure at xanthan concentrations above the overlap concentration[17].

The chemical stability of xanthan seems to be closely linked to its conformation. In general, high ionic strengths, which stabilize the ordered, double-stranded conformation, decrease the rates of degradation (measured as loss of viscosity) for both free-radical depolymerization and acid-catalysed hydrolysis[11,18,20]. In particular, a large increase in the degradation rate was observed when temperature approached[20] the estimated T_m. It was further noted[20] that, after 20 days (at a temperature slightly above the estimated T_m), the viscosity decay-constant changed from a constant value to lower values (more rapid degradation), possibly reflecting a conformational change. Another "anomaly" observed during the degradation of xanthan was a temporary increase in the viscosity following the initial decrease[21]. This was interpreted as a partial "melting" of the double-stranded structure, leading to an increased specific hydrodynamic volume[21].

Not only the conformational state, but also the chemical composition may change during degradation. For long-term treatment at high temperature in sea water, the mannose:glucose ratio[22] and pyruvate content[23] decreased, suggesting more rapid degradation in the side chains than in the main chain. Changes in the chemical composition may also influence the conformational properties and thus, stability. Therefore, monitoring changes in chemical composition as well as the conformational state are required for the analysis of biopolymer stability and interpretation of the results.

In addition to long-time storage of xanthan at elevated temperatures[20,22] stability studies may be performed by using accelerated degradation. Several methods are possible. It is assumed that free-radical degradation, mainly through the hydroxyl radical (OH·), is responsible for the observed degradation of biopolymers in oil-field applications[24]. Accelerated free-radical degradation of biopolymers is possible by gamma-radiolytic or photolytic techniques[19], or by adding reagents that generate hydroxyl radicals, such as hydrogen peroxide[25,26]. However, the precise reaction mechanisms and specificities against various linkages in polysaccharides are generally unknown[27]. An alternative method for polysaccharides is acid hydrolysis, because of known mechanisms and its widespread use in structure analysis. We therefore wished to adapt this method to studies on the degradation of xanthan. Furthermore, the stability of xanthan in acids is also of practical importance in certain oil-field operations, such as acidizing.

In the case of xanthan, a special type of behaviour is observed at low pH. The intrinsic viscosity is decreased ~20–30%, fully reversibly, on going from pH 7 to 2 in

10mM NaCl, but data on molecular weight, radius of gyration, and intrinsic viscosity has been interpreted in favour of maintaining the double-stranded structure, although in a more "semiflexible" conformation[28]. It should further be noted that the intrinsic viscosities of the same samples were totally independent of the ionic strength[29] when the latter was >10mM, even though a more-pronounced dependence of the intrinsic viscosity upon the ionic strength has been observed by others[30,31]. Optical rotation data also show that T_m shifts to higher values when the xanthan molecule is neutralized and, for fully neutralized xanthan, essentially no transition is observed[32] up to 80°.

Here we investigate the behaviour and degradation of xanthan in dilute acid (pH 1–4) at 80° at high (0.5M) and low (0.01M) ionic strength, using the intrinsic viscosity at low shear-rates to monitor the degradation process. Results are compared to optical rotation data obtained in the process of degradation and to the chemical composition of the degradation products as monitored by g.l.c. (following methanolysis) and by n.m.r. spectroscopy.

MATERIALS AND METHODS

Materials. — Xanthan (Kelzan XCD or Keltrol, Kelco, Inc., 1.0 mg/mL) in 10mM NaCl was stirred overnight at 20–22° and then filtered (0.8-μm filter). Portions of the stock solution were adjusted to the desired ionic strength by the addition of solid NaCl and then to the desired pH by the addition of 0.1M HCl. Xanthan solutions at pH 2.0 were obtained by dialysis against pure HCl solutions at pH 2.00 or against 0.5M NaCl adjusted to pH 2.00 with HCl. Solutions at pH 1.00 were obtained by adding HCl to the pH 2 solutions.

Samples used in the initial optical activity studies were prepared by dissolving xanthan (5 mg/mL) in 10mM NaCl. The solution was placed on an ice bath and sonicated for 10 min (400 W). The sonicated sample was centrifuged at 90 000 × g for 2 h at 20°, and the pellet was discarded. The supernatant solution was divided into separate fractions and each fraction was adjusted to the desired pH and ionic strength by dialysis. Samples were filtered through a filter with porosity 0.22 μm before measuring the optical rotation.

Hydrolyses. — The hydrolyses were performed at 80° in 100- or 500-mL Pyrex bottles with Teflon-lined caps. The concentration of xanthan was 1 mg/mL. Samples were taken at regular intervals and cooled to room temperature, using identical heating/cooling procedures in order to minimize possible hysteresis effects. About one half of each sample was adjusted to pH 6–7 with dilute NaOH. Selected samples were dialysed against 10mM HCl or 10mM NaCl, concentrated to 2–5 mg/mL using a Centriprep 10 concentrator (Amicon), and investigated by optical rotation as a function of temperature.

Analyses. — The intrinsic viscosity was determined at 3.3 s^{-1} with a Cartesian–diver viscometer[33,34]. The concentration ranges used corresponded to relative viscosities in the range of 1.1–2.5.

Optical activity was measured at 365 nm in a 10-cm cell thermostated by a circulating-water bath (Haake D8-G). The wavelength was 365 nm. A personal computer was used for automatic data acquisition as well as for temperature control. Data were calculated as the specific rotation, corrected for minor changes in sample volume at high temperatures.

The concentration of xanthan was determined by the phenol–sulfuric acid method[35] using a pyruvate- and acetate-free xanthan[36] as the standard.

The chemical composition of various degraded xanthans was determined by gas chromatography following methanolysis and silylation[37,38]. The samples were thoroughly dialysed against distilled water and freeze-dried. Polysaccharide (80–150 μg) and 10 μg *myo*-inositol (internal standard) were transferred to 1-mL acid-washed vials (Chromacol 1.1-STV, Chromacol Ltd., U.K.) and dried for 12 h *in vacuo* over fresh P_2O_5. Freshly made M methanolic HCl (Instant Methanolic HCl kit, Alltech Associates, Inc., U.S.A. 0.5 mL) was added and the vials were flushed with N_2 and sealed (Teflon-faced septa and screw caps). The vials were heated at 80° (± 1°) for 24 h, cooled to ambient temperature, and blown dry in a stream of nitrogen. The samples were finally dried for 12 h *in vacuo* over KOH pellets. Silylation was performed by adding 50 μL of Sylon HTP (Sigma Chemical Company, U.S.A.) followed by vigorous shaking. The reaction was allowed to proceed a minimum of 30 min before the vials were gently centrifuged to remove small amounts of a cloudy precipitate. The supernatants (0.5–1.5 μL) were injected into a gas chromatograph equipped with a split/splitless injector (split ratios 1:10–1:20) and flame-ionization detector. Injector and detector were both heated to 250°. The separation was performed on a fused-silica glass capillary column (CP-Sil-5-CB, 30 m, Chrompak, UK) using a temperature gradient (140–200°, 4°/min).

The chromatograms, showing only baseline-resolved peaks, were recorded and integrated on a digital integrator. Methanolysis yielded multiple peaks for each monosaccharide, and best results for quantification of component sugars was obtained by using the total peak area for each sugar.

The content of *O*-acetyl groups and pyruvate was determined by n.m.r. spectroscopy[11].

RESULTS

Conformation of xanthan at low pH. — Fig. 1 shows the specific optical rotation of xanthan as a function of temperature for a neutral solution (ionic strength 10 and 500mM) and at pH 3.0 and 3.9 (ionic strength 10mM). The values of the ionic strengths include contributions from added HCl. The effect of decreasing the pH is similar to the effect of increasing the ionic strength, namely the typical order–disorder transition-curve[3,7] shifts to progressively higher temperatures. At an ionic strength of 10mM T_m increased from 66 to 82° when going from neutral solution to pH 3.9, whereas at pH 3.0, which is close to the reported pK_a value of xanthan[40], no transition was observed below 100°. Below pH 3, there was no effect on $[\alpha]_{365}$ upon increasing the ionic strength (< 100°, not shown in Fig. 1). Based on the relationship between the specific optical rotation and

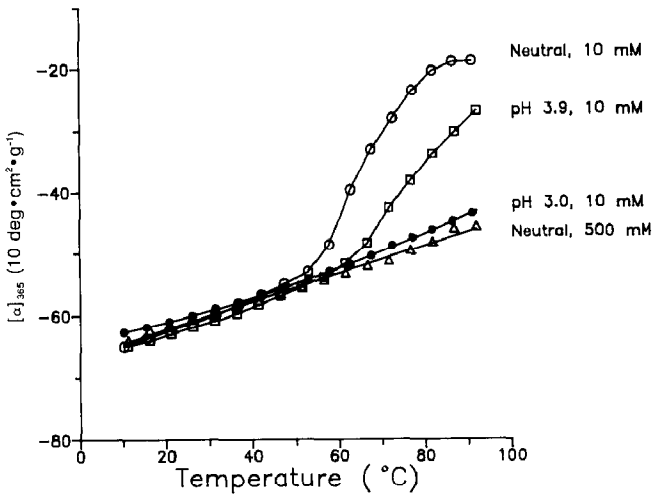

Fig. 1. Temperature dependence of the specific optical rotation ($[\alpha]_{365}$) for xanthan (degraded by sonication). The ionic strength was kept constant at 10mM at pH values of 6–7 (○), 3.9 (□), and 3.0 (△) and at 500mM at pH 6–7 (●).

the degree of order[5,17] the data indicate that, at pH 4 and ionic strength of 10mM, xanthan was initially about 50% disordered at 80°. For the other samples (pH 2.9 and 3.0) full order prevailed at the beginning of the degradation, irrespective of the ionic strength.

Intrinsic viscosity of hydrolysed xanthan. — The intrinsic viscosities of cooled and neutralized samples taken at various times during the degradation at 80° are shown in Fig. 2. The ionic strengths used during the viscosity measurements were the same as in the preceding hydrolyses (10 or 500mM). In all cases the data could be fairly well described by a single exponential-decay constant (Table I). The pH of the solutions at pH 4 and 3, but not at pH 2, showed a slightly drop early in the experiment, but remained constant thereafter (Table I).

At low ionic strength (10 mM), xanthan was most rapidly depolymerized at pH 4. There was no significant difference between the viscosity decay-constants at pH 2 and 3. At high ionic strength (500mM), the situation changed: the stability was highest at pH 4,

TABLE I

Viscosity decay-constants ($\tau = -1/k$ where k is the slope of $\ln([\eta]/[\eta]_0)$ versus time for xanthan at 80°

Initial pH	*Final pH*	*Ionic strength (M)*	*Decay constant (day)*
4.0	3.81	0.01	2.0
4.0	3.75	0.5	10.4
3.0	2.92	0.01	3.9
3.0	2.94	0.5	6.6
2.0	2.0	0.01	3.7
2.0	2.0	0.5	6.7
1.0	1.0	0.1	1.4

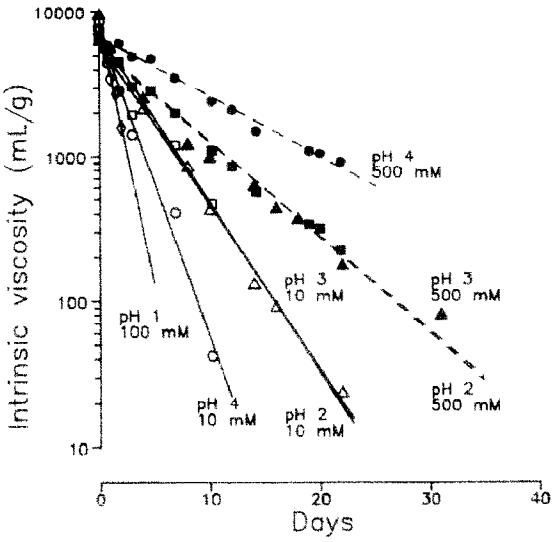

Fig. 2. Decrease in intrinsic viscosity $[\eta]$ upon hydrolysis of xanthan at 80° at pH 1 (◇), pH 2 (▲ △), pH 3 (■ □), and pH 4 (● ○) at ionic strengths of 10mM (filled symbols) or 500mM (open symbols) except at pH 1, where the ionic strength was 100mM. The samples were neutralized before measuring $[\eta]$.

and again with the same decay constants for pH 2 and 3. For all pH values, an increase in the ionic strength from 10 to 500mM resulted in increased stability, with the largest effect being observed at pH 4.

Heating/cooling effects may also influence the measured $[\eta]$ values. However, this effect is generally small, especially when compared to the range of $[\eta]$ values obtained by degradation (> 2 decades)[1].

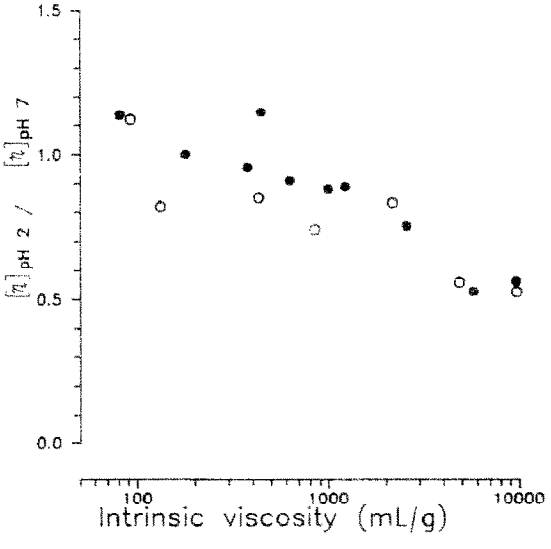

Fig. 3. Ratio between intrinsic viscosities before and after neutralization for xanthan degraded at pH 2. I = 10mM (●) and I = 500mM (○)

In addition to the neutralized samples, the intrinsic viscosities of some unneutralized samples were measured. For the series degraded at pH 2.0, the ratio between the intrinsic viscosities for unneutralized (pH 2) and neutralized (pH 7) increased monotonously from 0.54 and approached unity for the most-degraded samples (Fig. 3).

Chemical composition of partially hydrolysed xanthan. — Samples degraded at pH 1–4 were dialysed against distilled water, freeze-dried and the relative sugar composition was analysed by g.l.c. following methanolysis and silylation. The results are given in Fig. 4 and Table II. In all cases the ratio of glucuronic acid to glucose was essentially constant for the hydrolysis times investigated. For mannose the situation was different. From an initial mannose-to-glucose ratio of 1.0 this value decreased rapidly and approached the glucuronic acid-to-glucose ratio. First-order kinetics was followed for mannose-to-glucose ratios > 0.6, and the calculated rate-constants are given in Table II. The rate constants obtained at pH 2.0 at two different ionic strengths (10 and 100mM) were not significantly different. The data seem to deviate from strict proportionality between the rate constants and the concentration of protons, although the rates increase

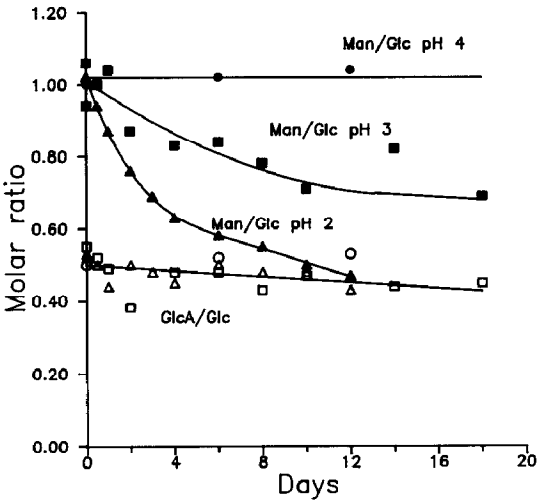

Fig. 4. Changes in the mannose/glucose- (filled symbols) and glucuronic acid/glucose-(open symbols) ratios of xanthan (non-dialysable fraction) during hydrolysis at 80° at pH 2.0 (▲ △), pH 3.0 (■ □), and pH 4.0 (● ○)

TABLE II

First-order rate-constants for the loss of mannose and glucuronic acid upon hydrolysis of xanthan at 80°, pH 1–3. The units are days^{-1}

pH	*Ionic strength* (M)	k'_{Man}	k'_{GlcA}
1.0	0.1	0.38	0.016
2.0	0.01	0.12	0.0090
2.0	0.1	0.096	0.0073
3.0	0.1	0.034	0.0088

by lowering the pH. N.m.r. analysis of a sample degraded for only 24 h at pH 2.0 showed a complete loss of both pyruvate and acetate.

Order–disorder transition of partially hydrolysed xanthan. — The temperature dependence of the optical rotation of xanthans hydrolysed at pH 2.0 was investigated. The results are given in Figs. 5 and 6 and in Table III. None of the samples displayed any detectable transition measured at pH 2, but the curves shifted to higher values of $[\alpha]_{365}$ at increased hydrolysis times (Fig. 5). Following neutralization (ionic strength of 10mM, Fig. 6), a transition was seen for the sample which was degraded for 8 days, with T_m = 68°, essentially the same as for unhydrolysed xanthan. At 100mM, this sample was fully ordered <95° (not shown in Fig. 6). For the sample degraded for 20 days, no transition was observed, but the $[\alpha]_{365}$ values were larger than those of less-degraded xanthan in the disordered state, with identical curves at ionic strengths of 10 and 100mM, respectively.

TABLE III

Chemical composition and thermally induced conformational change of xanthan degraded at pH 2

Degr. time	D_{Py}	D_{Ac}	*Man/Glc*	*GlcA/Glc*	$[\eta]$ (mL/g) *pH 2*	*pH 7*	T_m (I = 10mM) *pH 2*	*pH 7*
0 days	[a]	[a]	1.00	0.50	5100	7600	[b]	66
8 days	0	0	0.70	0.50	790	1070	[b]	68
20 days	0	0	0.45	0.39		37	[b]	[b]

[a] Not determined. [b] No transition detected.

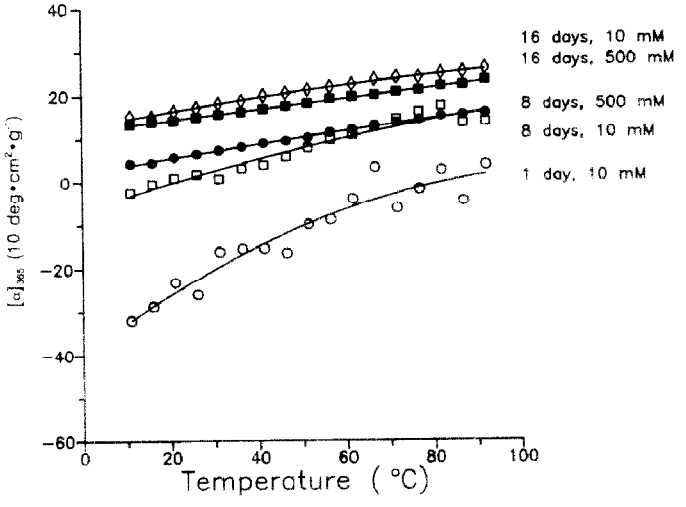

Fig. 5. Temperature dependence of the specific optical rotation ($[\alpha]_{365}$) for unneutralized xanthan degraded at pH 2.0, I = 10mM for 1 day (○), 8 days (□), and 16 days (◆), and at pH 2.0, I = 500mM for 8 days (●) and 16 days (■) days.

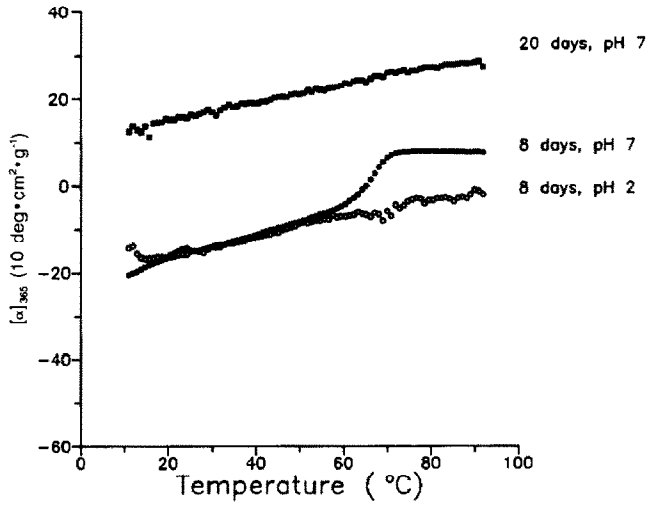

Fig. 6. Temperature dependence of the specific optical rotation ($[\alpha]_{365}$) for xanthan degraded at pH 2.0, I = 10mM for 8 days (○ ●) and 20 days (■). Measurements were performed at I = 10mM at pH 2 (open symbols) or pH 7 (filled symbols).

DISCUSSION

Mild acid hydrolysis of xanthan leads not only to depolymerization of the (1→4)-linked β-D-glucan backbone, but also to large changes in chemical composition because of hydrolysis in the side chains (Fig. 4, Table II). The results are expressed as molar ratios of mannose and glucuronic acid relative to glucose, as all analyses were performed on samples of high molecular weights ($[\eta] > 50$ mL/g). The rate constants given in Table II refer to the net losses of mannose and glucuronic acid, respectively. As hydrolysis of any residue in the side chain yields dialysable fragments, which were removed before analysis, the observed rate-constants may be expressed as follows:

$$k'_{GlcA} = k_{GlcA} + k_{\alpha\text{-Man}} \quad (1)$$

$$k'_{Man} = k_{\beta\text{-Man}} + k_{GlcA} + 2k_{\alpha\text{-Man}} \quad (2)$$

where k' values are the observed rate-constants (Table II), and the k values correspond to hydrolysis of each of the three residues in the side chain. From Eq. *(1)* we see that $k_{\alpha\text{-Man}} \leq k'_{GlcA}$. Thus, at pH 1 and 2, where $k'_{Man} >> k'_{GlcA}$, Eq. *(2)* yields:

$$k'_{Man} \simeq k_{\beta\text{-Man}} \quad (2b)$$

Hence, $k_{\beta\text{-Man}} >> k_{\alpha\text{-Man}}$. This difference may be due to two different effects. First, the α-mannose–glucose linkage may be less accessible to hydrogen ions or water, which adds to the mannose following heterolysis[41]. Secondly, the β-D-mannose, which is linked to O-4 of the glucuronic acid, may be subject to intramolecular hydrolysis[41,42]. For

uronic acid oligomers derived from alginate it has been suggested that intramolecular hydrolysis dominates near the pK_a, with a maximum[42] at a pH between pK_a and $pK_a - 1$. The uncertainty in the determination of k'_{GlcA} precludes, however, that the pH-dependence of the ratio k'_{Man}/k'_{GlcA} can be used as a further indication of intramolecular hydrolysis.

The g.l.c. analysis does not give information about the hydrolysis rates in the glucan backbone. Analysis of the intrinsic-viscosity data may allow a rough estimation of the number of broken bonds in the glucan backbone, and hence the first-order rate constant k_{Glc}, provided that an appropriate model is used. As a first approximation we have chosen the simplest model, namely, that xanthan is a linear, single-stranded polymer. This analysis may also provide further information in support of either a single-stranded, or indirectly, a multiple-stranded conformation. For random depolymerization, the weight average degree of polymerization (x_w) initially varies with time as described by the following equation[43]:

$$1/x_w = 1/(x_w)_0 + \tfrac{1}{2}kt \qquad (4)$$

where k is the first-order rate-constant for breaking a glycosidic bond in the glucose backbone, and x_w equals M_w/M_0, were M_0 is the average molecular weight per glucose residue. Eq. 4 requires that the fraction of broken bonds be very small compared to unity. This criterion is met even for the most-degraded samples, since intrinsic viscosities of 50–100 mL/g corresponds to molecular weights of xanthan in the range of 10^5. The value of M_w is directly related to the intrinsic viscosity $[\eta]$, for instance through the Mark–Houwink equation ($[\eta] = KM_w^a$). However, as the exponent a is not constant in the high-molecular-weight range, the $[\eta]$–M_w relationship is more conveniently described in terms of a semiflexible rod or wormlike chain. By setting $M_0 = 500$ and using the $[\eta]$–M_w relationship presented by Sato *et al.*[44], we obtain M_w and hence, $1/x_w$. Plots of $1/x_w$ versus time are shown in Fig. 7. Except for the sample degraded at pH 4 (I = 500mM), which covers a limited range of molecular weights, all curves deviate significantly from straight lines. Further, by using the slopes of the lines in Fig. 7 to calculate apparent k_{Glc}-values (Eq. 4), we obtain rate constants about 2–3 orders of magnitude lower than k'_{GlcA}, and hence, $k_{1\text{-}Man}$ (at pH 2 and 3). These data alone suggests that the glucan backbone is protected towards hydrolysis, especially in the initial phase. However, the deviations from straight lines in Fig. 7 clearly indicate that the single-stranded model for ordered xanthan is incompatible with the observed data. Rate constants derived from instrinsic-viscosity measurements do probably not correspond to the "real" hydrolysis rates. These may be higher, but the conformational state of xanthan may "mask" breaks in the glucan backbone when viscosity is used to monitor backbone depolymerization[11,12].

The hydrolysis of xanthan in dilute acid also exhibits significant deviations from the general acid-catalysed degradation of polysaccharides. First, the rate of degradation of the xanthan backbone, measured as intrinsic-viscosity decay, is apparently not proportional to the concentration of hydrogen ions. For instance, xanthan is more

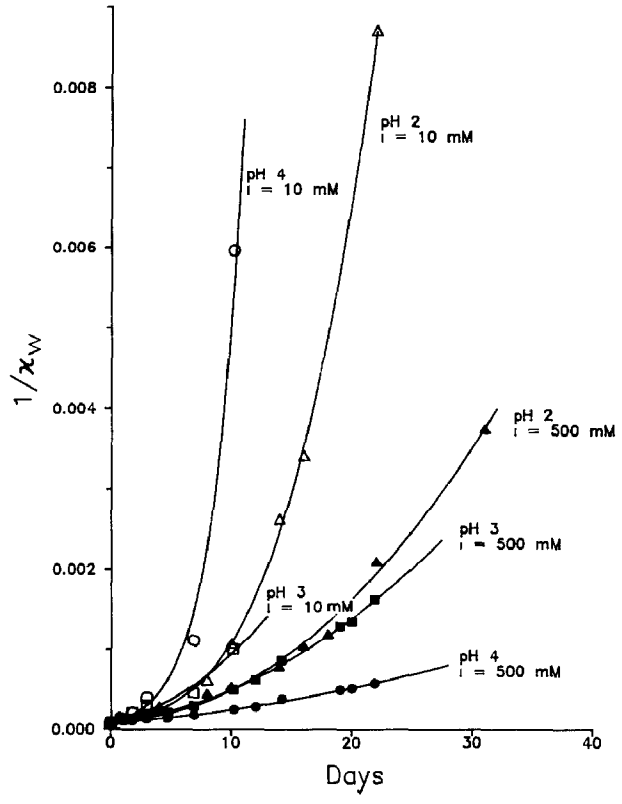

Fig. 7. Plot of $1/x_w$ (calculated from $[\eta]$) versus time for hydrolysis of xanthan at 80° at pH 2 (▲ △), pH 3.0 (■ □), pH 4.0 (● ○) at ionic strengths of 10mM (filled symbols) or 500mM (open symbols).

rapidly degraded at pH 4 than at pH 2 at low ionic strength (10mM). Secondly, the rate of degradation apparently increases with time, especially when $[\eta]$ falls below 500–1000 mL/g (Fig. 7). Finally, by increasing the ionic strength from 0.01 to 0.5, the degradation proceeds more slowly for all the pH values investigated, with the largest effect being at pH 4, which becomes the most stable pH.

A more-detailed analysis of the thermal stability of xanthan can only be performed by taking into consideration the special conformational behaviour of xanthan. Our data (Fig. 1) support those reported by others[3,32], namely a gradual shift of the apparent T_m towards higher temperatures as the pH and, hence, the degree of ionization, decreases. It was also confirmed that the intrinsic viscosity of undegraded xanthan shows a reversible decrease upon acidification[28]. However, for partially degraded xanthans, the difference gradually disappears upon prolonged degradation, which is in agreement with data on sonicated xanthan[28]. From the data in Fig. 1 and the literature already cited, it may be concluded that the hydrolysis experiments started with fully ordered xanthan, except at pH 4 and low ionic strength, where xanthan was ~50% disordered. As kinetic data for the depolymerization of ordered xanthan do not fit the single-stranded model, we next consider the behavior expected for a double-stranded model.

A single break in one of the chains in a double-stranded structure may not necessarily lead to an overall change in the hydrodynamic properties due to interchain stabilization. Also if both chains are broken, but with a certain distance between the two points, the structure may not lose its viscosity or measured molecular weight. This may happen provided that the distance is large enough to stabilize the double-helix conformation, an effect which indeed has been observed for DNA[45]. In the latter case, the molecular weight was virtually unaltered in the early phase of enzymic hydrolysis, despite a constant rate of chain cleavage, and it was estimated that the maximum number of contiguous hydrogen-bonds which fail to keep two fragments united was[45] at 2 pairs at 25°. A similar analysis may in principle be performed on xanthan, but requires accurate and direct measurement of the number of hydrolysed bonds in the glucan backbone. The data in Fig. 7, showing an increase in the degradation rate of ordered xanthan, are at least in qualitative agreement with a double-stranded model. A separate analysis could also answer whether or not these linkages are stabilized against hydrolysis because of their existence in an ordered, chain structure. The reaction mechanism for acid hydrolysis of glycosides[41] suggest that such a stabilization may take place because of steric hindrance in adopting the half-chair conformation of the intermediate carbonium ion, and because of the proximity of the carbonium ion to hydroxyl groups at the newly formed non-reducing end.

Another consequence of the "DNA-model" for xanthan may be predicted when the length of ordered fragments approach the critical length necessary to keep two chains together. Such fragments may denature into single strands, and the system eventually approach single-strand kinetics (Eq. 4). The contributions from double-stranded fragments containing long "sticky ends" is uncertain, but should be included for a more-detailed analysis. However, data on the most degraded samples in Fig. 7 may suggest that xanthan approaches single strand degradation kinetics.

An additional factor that requires consideration is the observed change in chemical composition. For instance, hydrolysis at pH 2 for up to 10 days at 80° left the glucuronic acid nearly uncleaved and, hence, the α-mannose almost unhydrolysed, whereas the amount of mannose was decreased by 50%. This result demonstrates the preferential hydrolysis of the outer β-mannose. The resulting polymer (obtained after 10 days, with an intrinsic viscosity as high as 500 mL/g) must be very similar to the so-called "polytetramer", a variant of xanthan lacking the outer β-mannose and which has been obtained by genetic manipulation of xanthan-producing bacteria[46]. Little is thus far known about the conformational behaviour and M_w–$[\eta]$ relationship of this polysaccharide, but X-ray fibre-diffraction studies of the "polytetramer" have suggested that the ordered structure is similar to that of intact xanthan[47]. The samples produced at pH 3 also lost some of the β-mannose, but never reached the "polytetramer" state in this experiment. At pH 4, changes the sugar composition of xanthan could not be detected, despite a substantial loss of viscosity at low ionic strength. Similar changes in the sugar composition of xanthan were observed upon degradation by long-term treatment in sea water[22] at ambient pH, although the structure–conformation relationship was not further investigated. A comparison of the data obtained at pH 2 and 3 (where the rates

of intrinsic viscosity losses were essentially equal, despite the much more rapid loss of β-mannose at pH 2) indicates that the removal of the outer mannose at least does not increase the decay of intrinsic viscosity at these pH-values. A tentative explanation is that the β-mannose is not essential in maintaining the ordered conformation of xanthan.

The change in chemical composition also changes the molar mass of xanthan and, in principle, influences the xanthan concentrations used in calculating the intrinsic viscosities. Selective removal of the β-mannose decreases the polymer concentration by ~20%, with a corresponding increase in the calculated intrinsic viscosity. However, as xanthan is an extremely stiff molecule in its ordered state, we assume that changes in the side chains do not influence the hydrodynamic volume when compared to the effects of backbone depolymerization. In order to obtain intrinsic viscosities and molecular weights that allow a comparison between the depolymerization rates of xanthans of variable chemical compositions, the intrinsic viscosities were calculated on the basis of a constant chemical composition (intact "pentamer") throughout the hydrolysis process.

An investigation of the conformational properties of some of the xanthans degraded at pH 2 was performed by using a standard optical-rotation method (Table III). When measured at pH 2, where the hydrolysis took place, no thermally induced transition could be detected at any time in the degradation process (Fig. 5). In this case, a continuous increase in the absolute value of [α] was observed with increasing hydrolysis times, starting at values for undegraded xanthan corresponding to ordered xanthan and ending in the range of disordered xanthan. This change may be attributed to an increasing fraction of disordered xanthan[5], which is in concordance with the viscosity behaviour. It is also possible that the preferential loss of β-mannose shifts [α] to larger values, as also observed for galactomannans with variable contents of β-mannose[48]. However, an increase in [α] has also been observed for sonicated xanthan[5], even though this procedure is thought to degrade only the backbone of xanthan. After 8 days of hydrolysis at pH 2, the *neutralized* sample still exhibited the normal order-disorder transitions upon heating (Fig. 6). The value of T_m (at 10mM ionic strength) was essentially the same as for undegraded xanthan (Table III), again suggesting that the "polytetramer" behaves in a manner similar to normal xanthan with respect to the order–disorder transition. A sample degraded for 20 days at pH 2 behaved like disordered xanthan, both before and after neutralization. The absence of a transition was also confirmed by differential scanning calorimetry (A. Flaibani, personal communication).

The difference in intrinsic viscosities measured at pH 2 and 6–7 gradually disappears upon degradation at pH 2 (Fig. 3), which also suggests that the effect of pH upon the conformational behaviour becomes less important during the hydrolysis.

The hydrolysed xanthans described in this work appear to be promising model substances for structure–function relationship. In contrast to the "pentamer–tetramer–trimer" series of xanthan[46], with large and discrete differences in chemical composition, hydrolysis may produce a continuous series of modified xanthans along the "pentamer–trimer" gradient. This is possible because of the effective retention of intrinsic viscosity upon acid hydrolysis.

ACKNOWLEDGMENTS

This work was financed by the Royal Norwegian Council for Industrial and Scientific Research (Project BT.16.23484) and Statoil (VISTA-grant V6314).

REFERENCES

1 P. E. Jannson, L. Kenne, and B. Lindberg, *Carbohydr. Res.*, 45 (1975) 275–282.
2 I. W. Sutherland, *Carbohydr. Res.*, 131 (1984) 93–104.
3 G. Holzwarth, *Biochemistry*, 15 (1976) 4333–4339.
4 E. R. Morris, D. A. Rees, G. Young, M. D. Walkinshaw, and A. Darke, *J. Mol. Biol.*, 110 (1977) 1–16.
5 W. Liu and T. Norisuye, *Int. J. Biol. Macromol.*, 10 (1988) 45–50.
6 I. T. Norton, D. M. Goodall, S. A. Frangou, E. R. Morris, and D. A. Rees, *J. Mol. Biol.*, 175 (1984) 371–394.
7 W. Liu, T. Sato, T. Norisuye, and H. Fujita, *Carbohydr. Res.*, 160 (1987) 267–281.
8 A. J. Clarke-Sturman, J. P. Pedley, and P. L. Sturla, *Int. J. Biol. Macromol.*, 8 (1986) 355–360.
9 M. Milas, M. Rinaudo, and B. Tinland, *Carbohydr. Polym.*, 6 (1986) 95–107.
10 G. Holzwarth and J. Ogletree, *Carbohydr. Res.*, 76 (1979) 277–280.
11 P. Foss, B. T. Stokke, and O. Smidsrød, *Carbohydr. Polym.*, 7 (1987) 421–433.
12 T. Sato, S. Kojima, T. Norisuye, and H. Fujita, *Polym. J.*, 16 (1984) 423–429.
13 B. T. Stokke, A. Elgsæter, and O. Smidsrød, *Int. J. Biol. Macromol.*, 8 (1986) 217–225.
14 B. T. Stokke, A. Elgsæter, G. Skjåk-Bræk, and O. Smidsrød, *Carbohydr. Res.*, 160 (1987) 13–28.
15 M. Milas and M. Rinaudo, *Carbohydr. Res.*, 158 (1986) 191–204.
16 G. Muller, M. Anrhourrache, J. Lecourtier, and G. Chauveteau, *Int. J. Biol. Macromol.*, 8 (1986) 167–172.
17 D. M. Goodall, in W. Knoche and R. Schomäcker (Eds.), *Reactions in compartmentalized liquids*, Springer Verlag, Berlin, 1989, 153–162.
18 F. Lambert and M. Rinaudo, *Polymer*, 26 (1985) 1549–1553.
19 B. J. Parsons, G. O. Phillips, B. Thomas, D. J. Wedlock, and A. J. Clarke-Sturman, *Int. J. Biol. Macromol.*, 7 (1985) 187–192.
20 R. S. Seright and B. J. Henrici, SPE Paper No. 14946 (1986) 285–299.
21 K. Hatakenaka, W. Liu, and T. Norisuye, *Int. J. Biol. Macromol.*, 9 (1987) 346–348.
22 B. T. Stokke, P. Foss, B. E. Christensen, C. Kierulf, and I. W. Sutherland, *Int. J. Biol. Macromol.*, 11 (1989) 137–145.
23 C. Kierulf and I. W. Sutherland, *Carbohydr. Polym.*, 9 (1988) 185–194.
24 S. L. Wellington, *Soc. Pet. Eng. J.*, Dec. (1983) 901–912.
25 J. Weiss, *Adv. Catal.*, 4 (1952) 343–365.
26 O. Smidsrød, A. Haug, and B. Larsen, *Acta Chem. Scand.*, 19 (1965) 143–152.
27 K. Uchida and S. Kawakishi, *Carbohydr. Res.*, 173 (1988) 89–99.
28 L. Zhang, W. Liu, T. Norisuye, and H. Fujita, *Biopolymers*, 26 (1987) 333–341.
29 T. Sho, T. Sato, and T. Norisuye, *Biophys. Chem.*, 25 (1986) 307–313.
30 B. T. Stokke, O. Smidsrød, A. B. L. Marthinsen, and A. Elgsæter, in G. A. Stahl and D. N. Schultz (Eds.) *Water-Soluble Polymers for Petroleum Recovery*, Plenum Publ. Corp., New York, 1988, 243–252.
31 B. Tinland and M. Rinaudo, *Macromolecules*, 22 (1989) 1863–1865.
32 M. Nakasuga and T. Norisuye, *Polym. J.*, 20 (1988) 939–945.
33 B. T. Stokke, A. Mikkelsen, and A. Elgsæter, *Biochim. Biophys. Acta*, 816 (1985) 102–110.
34 A. Mikkelsen, B. T. Stokke, B. E. Christensen, and A. Elgsæter, *Biopolymers*, 24 (1985) 1683–1704.
35 M. Dubois, K. A. Gilles, J. K. Hamilton, P. A. Rebers, and F. Smith, *Anal. Chem.*, 28 (1956) 350–356.
36 M. Rinaudo, M. Milas, F. Lambert, and M. Vincendon, *Macromolecules*, 16 (1983) 816–819.
37 M. F. Chaplin, *Anal Biochem.*, 123 (1982) 336–341.
38 B. E. Christensen, J. Kjosbakken, and O. Smidsrød, *Appl. Environ. Microbiol.*, 50 (1985) 837–845.
39 Y. W. Ha and R. L. Thomas, *J. Food Sci.*, 53 (1988) 574–577.
40 M. Rinaudo and M. Milas, *Biopolymers*, 17 (1978) 2663–2678.
41 J. N. BeMiller, *Adv. Carbohydr. Chem.*, 22 (1976) 25–108.
42 O. Smidsrød, A. Haug, and B. Larsen, *Acta Chem. Scand.*, 20 (1966) 1026–1034.
43 C. Tanford, *Physical chemistry of macromolecules*, John Wiley & Sons, New York, 1961, pp. 611–624.

44 T. Sato, T. Norisuyc, and H. Fujita, *Macromolecules*, 17 (1984) 2696–2700.
45 C. A. Thomas, *J. Am. Chem. Soc.*, 78 (1956) 1861–1868.
46 R. W. Vanderslice, D. H. Doherty, M. A. Capage, M. R. Betlach, R. A. Hassler, N. M. Henderson, J. Ryan-Graniero, and M. Tecklenburg, in V. Crescenzi, I. C. M. Dea, S. Paoletti, S. S. Stivala and I. W. Sutherland (Eds.), *Biomedical and Biotechnological Advances in Industrial Polysaccharides*. Gordon and Breach Science Publ., New York, 1989, 145–156.
47 R. P. Millane and T. V. Narasaiah, *Carbohydr. Polym.*, 12 (1990) 315–321.
48 L. A. Buffington, E. S. Stevens, E. R. Morris, and D. A. Rees, *Int. J. Biol. Macromol.*, 2 (1980) 199–203.